Journal of
Mechanics of
Materials and Structures

POSTBUCKLING AND DELAMINATION GROWTH FOR DELAMINATED PIEZOELECTRIC ELASTOPLASTIC LAMINATED BEAMS UNDER HYGROTHERMAL CONDITIONS

Ying-Li Li, Yi-Ming Fu and Hong-Liang Dai

Volume 7, No. 1 January 2012

mathematical sciences publishers

JOURNAL OF MECHANICS OF MATERIALS AND STRUCTURES
Vol. 7, No. 1, 2012

POSTBUCKLING AND DELAMINATION GROWTH FOR DELAMINATED PIEZOELECTRIC ELASTOPLASTIC LAMINATED BEAMS UNDER HYGROTHERMAL CONDITIONS

YING-LI LI, YI-MING FU AND HONG-LIANG DAI

The postbuckling and delamination growth for delaminated piezoelectric elastoplastic laminated beams under hygrothermal conditions are investigated. By considering hygrothermal environments, transverse shear deformation, geometrical nonlinearity and piezoelectric effect, the incremental nonlinear equilibrium equations of the piezoelectric elastoplastic laminated beams with delamination are obtained. The finite difference method and iterative method are adopted to solve the equations. Based on these, the delamination growth for the piezoelectric elastoplastic laminated beams is studied using J-integral theory. In the numerical examples, the effects of hygrothermal environments, transverse shear deformation, geometrical nonlinearity and piezoelectricity on the postbuckling behavior and delamination growth for the delaminated piezoelectric elastoplastic laminated beams are discussed in detail.

1. Introduction

Piezoelectric laminated structures have great application potential in mechanical, aerospace, nuclear, reactor, and civil engineering, and in many modern industries due to their excellent properties. The challenge is that, during the manufacturing and service process, damage can arise that weakens the mechanical properties and reduce significantly the service life of the structure. Delamination is the main form of damage in laminated structures, and its growth has a detrimental influence on the behavior of the structure. The concentration of load-induced stress along the delamination front an cause delamination growth and ultimately lead to structural failure. At the same time, as structures can still bear loads after exceeding their yield limits, it is uneconomical to restrict structural design to the elastic regime. To make the best of the material, investigation should be extended to the mechanical properties in plastic stage.

Temperature and humidity variations cause hygrothermal stress, which also influences the performance of the piezoelectric composites. Consequently, it is important to analyze the postbuckling and delamination growth of delaminated piezoelectric elastoplastic beams by considering the effects of the hygrothermal conditions, transverse shear deformation, geometric nonlinearity, and the piezoelectric effect.

We mention some relevant studies. Davidson et al. [2000] analyzed energy release rates and stress intensity factors for delaminated composite laminates. Applying the finite element method, Nilsson et al. [2001] researched delamination buckling and growth in a slender composite panel. Park and Sankar [2002] and Wang and Qiao [2004] computed energy release rates of delaminated plates with the first-order shear deformable theory. A boundary layer theory of shell buckling was extended to the case of shear deformable laminated cylindrical panels under hygrothermal environments and a singular perturbation technique was employed to determine the buckling loads and postbuckling equilibrium paths in [Shen

Keywords: hygrothermal conditions, piezoelectric effect, postbuckling, delamination growth, J-integral.

2002; Shen 2001]. Tafreshi [2006] used the virtual crack closure technique to find the distribution of the local strain energy release rate along the delamination front. Münch and Ousset [2002] developed a numerical method to simulate delamination growth in layered composite structures within the framework of fracture mechanics in large displacement.

Much research has been conducted in elastoplastic mechanics. But most existing elastoplastic models are based on Hill's yield criterion, which suppose the material yield is independent of the spherical stress tensor. Actually, under the acting of the spherical stress tensor, the structures will be distorted due to the different elastic constants in each principal direction. According to the von Mises distortion energy yield criteria, the materials will get into the plastic stage if the distortion energy reaches a certain value, and the materials have apparent Bauschinger effect under the action of the stresses. Hence, Hill's hypothesis is inconsistent with the practical situation. Against the flaw mentioned above, Yuan and Zheng [1990] established a new yield criterion that relate to the spherical stress tensor, and obtained the associated plastic flow law for the elastoplastic material. Pi and Bradford [2003] investigated elastic and elastoplastic flexural–torsional buckling and postbuckling behavior of arches that are subjected to a central concentrated load by using the rational finite element model.

In order to analysis the growth of the delamination, we have to get a clue of the stress field along the delamination front. Rice [1968] proposed the J integral theory in 1968 and used an integral to describe the intensity of the stress and strain field in the vicinity of the crack tip of elastoplastic structure. Yang et al. [2002] studied the theory of J integral near crack tip in the plate of linear-elastic orthotropic composite material by using a complex function method. Simha et al. [2008] discussed the crack driving force in elastic–plastic materials, with particular emphasis on incremental plasticity, by using the configurational forces approach and standard constitutive models for finite strain. Based on the law of conservation of energy, the generalized piezoelectric J integral was defined in [Pak and Herrmann 1986; Pak 1990; Zuo and Sih 2000], including piezoelectric effects and was proved to be unaffected by the choice of a contour. However, up to now, the analysis of delaminated piezoelectric elastoplastic laminated beams is still open.

This paper aims to study the postbuckling behavior and energy release rate of the delaminated piezoelectric elastoplastic laminated beams and investigate the effects of hygrothermal conditions, transverse shear deformation, geometric nonlinearity and piezoelectricity on their behavior. The incremental theory of elastoplastic is employed to derive the governing equations. The numerical solutions are obtained by using the finite difference method and the iteration method. Numerical simulations demonstrate the effects of the hygrothermal conditions, yield stress, piezoelectricity, slenderness ratio, delamination size, and delamination length on postbuckling behavior and energy release rate.

2. Elastoplastic constitutive models of mixed hardening orthotropic materials

In the case of the elastoplastic deformation, we make these assumptions:

(1) Spherical stress tensors produce plastic deformations, and plastic strains are compressible.

(2) Uniform dilatation produced by active stresses will not influence the plastic deformation.

(3) The yield surface moves and expands along with plastic deformation.

(4) The dimensionless yield criterion of orthotropic material is isomorphic with the von Mises criterion of isotropic material.

Based on there assumptions, Tian et al. [2009] defined the dimensionless yield function as

$$f = \frac{K^2}{2}\left[(\tilde{\sigma}_{11}^{'} - \tilde{\sigma}_{22}^{'})^2 + (\tilde{\sigma}_{22}^{'} - \tilde{\sigma}_{33}^{'})^2 + (\tilde{\sigma}_{33}^{'} - \tilde{\sigma}_{11}^{'})^2 + 2(\tilde{\sigma}_{44}^{'2} + \tilde{\sigma}_{55}^{'2} + \tilde{\sigma}_{66}^{'2})\right], \tag{1}$$

where

$$\tilde{\sigma}_{ij}^{'} = \frac{\sigma_{ij} - b_{ij}}{\Sigma_{ij}} \quad \text{(no sum over } i, j), \tag{2}$$

The constant K, with dimensions of stress, can be determined by experiments in the simple stress state; σ_{ij} and Σ_{ij} are the stress tensor and yield stress tensor components, respectively, along each direction of orthotropic materials; b_{ij} is the back stress tensor, which represents the transition of the center of the yield surface, and reflects the kinematics hardening.

By defining the effective active stress as

$$\tilde{\sigma} = \frac{K}{\sqrt{2}}\sqrt{(\tilde{\sigma}_{11}^{'} - \tilde{\sigma}_{22}^{'})^2 + (\tilde{\sigma}_{22}^{'} - \tilde{\sigma}_{33}^{'})^2 + (\tilde{\sigma}_{33}^{'} - \tilde{\sigma}_{11}^{'})^2 + 2(\tilde{\sigma}_{44}^{'2} + \tilde{\sigma}_{55}^{'2} + \tilde{\sigma}_{66}^{'2})}, \tag{3}$$

the mixed hardening yield function can be given as

$$F_p = f(\tilde{\sigma}_{ij}^{'}) - [\tilde{\sigma}(\bar{\varepsilon}^p)]^2, \tag{4}$$

where $\tilde{\sigma}$ is the effective stress defined in (3), which is the function of effective plastic strain $\bar{\varepsilon}^p$, and can be acquired by the simple extension experimental curves.

Assuming a non-associated flow rule, the plastic part of the strain tensor increment $d\varepsilon_{ij}^p$ is proportional to the gradient of the stress function F_p, commonly named plastic potential function

$$d\varepsilon_{ij}^p = \lambda_p \frac{\partial F_p}{\partial \sigma_{ij}} = \lambda_p \frac{\partial f}{\partial \sigma_{ij}}, \tag{5}$$

where λ_p is a non-negative scalar called plastic multiplier or consistency parameter.

Substituting (1) and (2) into (4), the following formulas can be obtained

$$\begin{aligned}
d\varepsilon_{11}^p &= \lambda_p \frac{K^2}{\Sigma_{11}}(2\tilde{\sigma}_{11}^{'} - \tilde{\sigma}_{22}^{'} - \tilde{\sigma}_{33}^{'}), \quad d\varepsilon_{44}^p = 2\lambda_p \frac{K^2}{\Sigma_{44}}\tilde{\sigma}_{44}^{'}, \\
d\varepsilon_{22}^p &= \lambda_p \frac{K^2}{\Sigma_{22}}(2\tilde{\sigma}_{22}^{'} - \tilde{\sigma}_{33}^{'} - \tilde{\sigma}_{11}^{'}), \quad d\varepsilon_{55}^p = 2\lambda_p \frac{K^2}{\Sigma_{55}}\tilde{\sigma}_{55}^{'}, \\
d\varepsilon_{33}^p &= \lambda_p \frac{K^2}{\Sigma_{33}}(2\tilde{\sigma}_{33}^{'} - \tilde{\sigma}_{11}^{'} - \tilde{\sigma}_{22}^{'}), \quad d\varepsilon_{66}^p = 2\lambda_p \frac{K^2}{\Sigma_{66}}\tilde{\sigma}_{66}^{'}.
\end{aligned} \tag{6}$$

Substituting (6) into (3), we have

$$\begin{aligned}
\tilde{\sigma} = \frac{1}{3\sqrt{2}K\lambda_p}\big((\Sigma_{11}d\varepsilon_{11}^p - \Sigma_{22}d\varepsilon_{22}^p)^2 + (\Sigma_{22}d\varepsilon_{22}^p - \Sigma_{33}d\varepsilon_{33}^p)^2 + (\Sigma_{33}d\varepsilon_{33}^p - \Sigma_{11}d\varepsilon_{11}^p)^2 \\
+ \tfrac{9}{2}[(\Sigma_{44}d\varepsilon_{44}^p)^2 + (\Sigma_{55}d\varepsilon_{55}^p)^2 + (\Sigma_{66}d\varepsilon_{66}^p)^2]\big)^{\frac{1}{2}}.
\end{aligned} \tag{7}$$

Define the effective plastic strain increment as

$$d\bar{\varepsilon}^p = \frac{\sqrt{2}}{3K}\big((\Sigma_{11}d\varepsilon_{11}^p - \Sigma_{22}d\varepsilon_{22}^p)^2 + (\Sigma_{22}d\varepsilon_{22}^p - \Sigma_{33}d\varepsilon_{33}^p)^2 + (\Sigma_{33}d\varepsilon_{33}^p - \Sigma_{11}d\varepsilon_{11}^p)^2 + \tfrac{9}{2}[(\Sigma_{44}d\varepsilon_{44}^p)^2 + (\Sigma_{55}d\varepsilon_{55}^p)^2 + (\Sigma_{66}d\varepsilon_{66}^p)^2]\big)^{\frac{1}{2}}. \quad (8)$$

According to (7) and (8), we obtain

$$d\bar{\varepsilon}^p = 2\tilde{\sigma}\lambda_p. \quad (9)$$

The plastic strain can be decomposed as

$$d\varepsilon_{ij}^p = d\varepsilon_{ij}^{p(\mathrm{I})} + d\varepsilon_{ij}^{p(\mathrm{II})}, \quad (10)$$

where $d\varepsilon_{ij}^{p(\mathrm{I})}$, the incremental plastic strain of isotropic hardening, and $d\varepsilon_{ij}^{p(\mathrm{II})}$, the incremental plastic strain of kinematics hardening, are defined by

$$d\varepsilon_{ij}^{p(\mathrm{I})} = a d\varepsilon_{ij}^p, \quad d\varepsilon_{ij}^{p(\mathrm{II})} = (1-a)\, d\varepsilon_{ij}^p. \quad (11)$$

Here a is the mixed hardening parameter within span $(-1, 1)$; the value $a = 1$ denotes pure isotropic hardening, and $a = 0$ denotes pure kinematic hardening. When a is negative, the yield surface shrinks. Other values denote mixed hardening. The incremental back stress tensor can be defined as a linear function of incremental plastic strain tensor of kinematics hardening:

$$db_{ij} = c d\varepsilon_{ij}^{p(\mathrm{II})}, \quad (12)$$

where c is the ratio constant. According to (5) and (11), the back stress increment can be expressed as

$$db_{ij} = c(1-a)\lambda_p \frac{\partial f}{\partial \sigma_{ij}}. \quad (13)$$

The total strain increment is decomposed into elastic and plastic strain increments:

$$d\varepsilon_{ij} = d\varepsilon_{ij}^e + d\varepsilon_{ij}^p. \quad (14)$$

The elastic constitutive equation is

$$d\sigma_{ij} = C_{ijkl}^e d\varepsilon_{kl}^e; \quad (15)$$

using (14) and (15), one gets

$$d\sigma_{ij} = C_{ijkl}^e \left(d\varepsilon_{kl} - \lambda_p \frac{\partial f}{\partial \sigma_{kl}} \right). \quad (16)$$

According to the consistency condition, and letting $H' = d\tilde{\sigma}/d\bar{\varepsilon}^p$, from (4), we have

$$\frac{\partial f}{\partial \tilde{\sigma}_{ij}'} d\tilde{\sigma}_{ij}' - 2\tilde{\sigma} H' d\bar{\varepsilon}^p = 0. \quad (17)$$

Substituting (5), (9), (13) and (16) into this, we obtain

$$\lambda_p = \frac{X_{ij} d\varepsilon_{ij}}{S}, \quad (18)$$

where

$$X_{ij} = \frac{1}{\Sigma_{kl}} \frac{\partial f}{\partial \tilde{\sigma}'_{kl}} C^e_{klij},$$
$$S = \frac{1}{\Sigma_{ij}} \frac{\partial f}{\partial \tilde{\sigma}'_{ij}} C^e_{ijkl} \frac{1}{\Sigma_{kl}} \frac{\partial f}{\partial \tilde{\sigma}'_{kl}} + \frac{1}{\Sigma_{ij}} \frac{\partial f}{\partial \tilde{\sigma}'_{ij}} c(1-\alpha) \frac{1}{\Sigma_{ij}} \frac{\partial f}{\partial \tilde{\sigma}'_{ij}} + 4\tilde{\sigma}^2 H'. \tag{19}$$

Substituting (18) into (16), the incremental elastoplastic constitutive equation can be written as

$$d\sigma_{ij} = (C^e_{ijkl} - C^p_{ijkl})\, d\varepsilon_{kl}, \tag{20}$$

where $C^p_{ijkl} = X_{ij} X_{kl}/S$. Therefore, the incremental elastoplastic constitutive equation of orthotropic materials is

$$d\sigma_{ij} = (C^e_{ijkl} - \chi C^p_{ijkl})\, d\varepsilon_{kl}. \tag{21}$$

If $F_p = 0$ and $\dfrac{\partial f}{\partial \sigma_{ij}} d\sigma_{ij} > 0$, then $\chi = 1$. If $F_p < 0$ or $\dfrac{\partial f}{\partial \sigma_{ij}} d\sigma_{ij} \le 0$, then $\chi = 0$.

3. Fundamental equations of delaminated piezoelectric laminated beams under hygrothermal conditions

Consider a delaminated piezoelectric laminated beam under an axial load P depicted in Figure 1. The delaminated piezoelectric laminated beam is composed of a fiber-reinforced laminated beam and the upper and lower piezoelectric layers. Take the piezoelectric layers as elastic layers and the fiber-reinforced laminates to be elastoplastic. The global coordinate system oxz is shown in Figure 1 and the reference

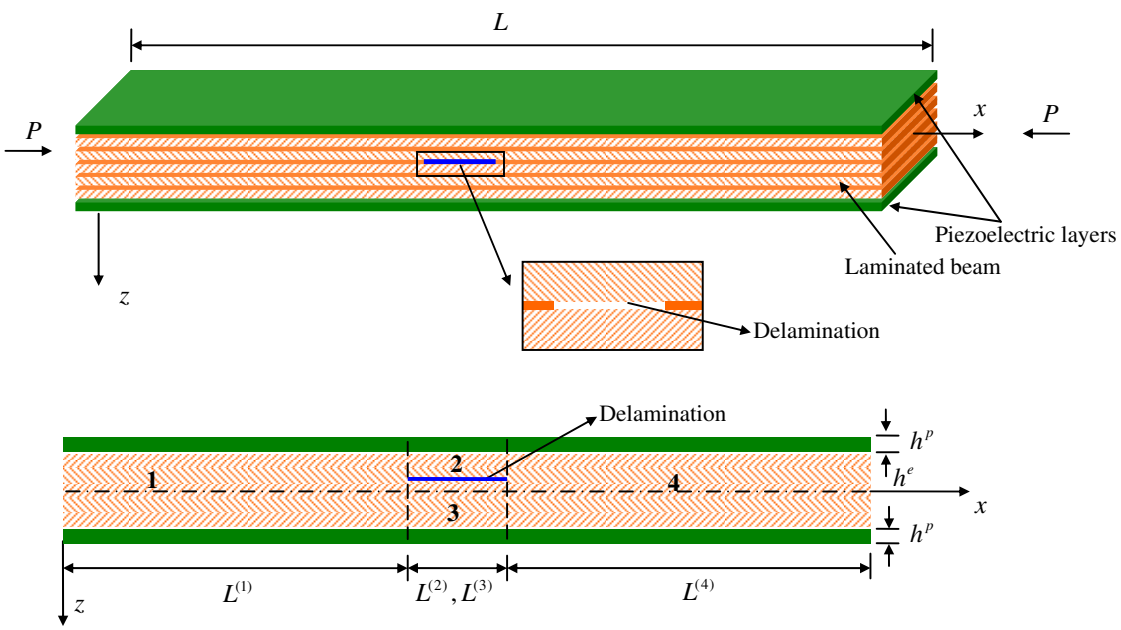

Figure 1. Geometric configuration (top) and transverse geometry (bottom) of piezoelectric laminated beam.

plane $z = 0$ is located at the midsurface of the undeformed laminated beams. The beam with throughout width delamination has length L, thickness h^e and delaminated length $L^{(2)}$. $L^{(1)}$ is the distance from the left end of the delamination to that of the beam. In order to investigate the delamination growth, the delaminated laminated beam is divided into four regions which are respectively denoted as $\Omega^{(i)e}$ $(i = 1, 2, 3, 4)$. Here the indices 2 and 3 represent the delaminated segments, while 1 and 4 represent the intact segments. The length of each region is defined as $L^{(i)}$, and the coordinate x for each region is measured from the left end. The thickness of regions 2 and 3 are $h^{(2)e}$ and $h^{(3)e}$ respectively, and obviously $h^{(2)e} + h^{(3)e} = h^e$. The piezoelectric layers with thickness h^p are perfectly bonded on the upper and lower surfaces of the laminated beam. The corresponding piezoelectric layers bonded on the regions $\Omega^{(i)e}$ are denoted by $\Omega^{(i)p}$. Then the whole piezoelectric laminated beam is divided into four regions denoted by $\Omega^{(i)}$, and $\Omega^{(i)} = \Omega^{(i)e} + \Omega^{(i)p}$. The coordinate system of every region $ox^{(i)}z^{(i)}$ is located at the midsurface of the related region. The thickness of the whole piezoelectric laminated beams is $h = h^e + 2h^p$.

Supposing $\bar{u}^{(i)}$, $\bar{w}^{(i)}$ denote the displacements of an arbitrary point in region $\Omega^{(i)}$ throughout the x, z direction, respectively, and $\phi^{(i)}$ denotes the angle the section rotate along the neutral axis, then the displacement components are given by

$$\begin{aligned} \bar{u}^{(i)}(x, z) &= u^{(i)}(x) + z\phi^{(i)}(x), \\ \bar{w}^{(i)}(x, z) &= w^{(i)}(x) + \tilde{w}^{(i)}(x), \end{aligned} \tag{22}$$

where $u^{(i)}$, $w^{(i)}$ are displacement components of the points on the midsurface. $\tilde{w}^{(i)}$ denotes the initial deflection and x, z is the coordinate of corresponding region.

If that $\bar{\varepsilon}_x^{(i)}$, $\bar{\varepsilon}_{xz}^{(i)}$ are the strains of an arbitrary point in region $\Omega^{(i)}$, the nonlinear strain-displacement relations can be written as

$$\bar{\varepsilon}_x^{(i)} = \varepsilon_x^{(i)} + z\kappa_x^{(i)}, \quad \bar{\varepsilon}_{zx}^{(i)} = \varepsilon_{zx}^{(i)}, \tag{23}$$

where $\varepsilon_x^{(i)}$, $\varepsilon_{xz}^{(i)}$ are the strains of the corresponding points on the midsurface, and $\kappa_x^{(i)}$ is the curvature, and

$$\varepsilon_x^{(i)} = u_{,x}^{(i)} + \tfrac{1}{2} w_{,x}^{(i)2} + w_{,x}^{(i)} \tilde{w}_{,x}^{(i)}, \quad \varepsilon_{zx}^{(i)} = w_{,x}^{(i)} + \phi^{(i)}, \quad \kappa_x^{(i)} = \phi_{,x}^{(i)} \tag{24}$$

where the comma denotes the derivative with respect to the coordinate.

When the load acting on the beam varies, the displacement and strains of an arbitrary point of the beam would alter accordingly. Then, the strain increments of the midsurface are

$$d\varepsilon_x^{(i)} = du_{,x}^{(i)} + \tfrac{1}{2} dw_{,x}^{(i)2} + (w_{,x}^{(i)} + \tilde{w}_{,x}^{(i)})\, dw_{,x}^{(i)}, \quad d\varepsilon_{zx}^{(i)} = dw_{,x}^{(i)} + d\phi^{(i)}, \quad d\kappa_x^{(i)} = d\phi_{,x}^{(i)}. \tag{25}$$

The incremental elastoplastic stress-strain relations of a single layer for the fiber-reinforced laminated beam in the local coordinate can be obtained as

$$\begin{Bmatrix} d\sigma_x^{(i)k} \\ d\tau_{zx}^{(i)k} \end{Bmatrix} = \begin{pmatrix} C_{11}^e - \chi C_{11}^p & C_{15}^e - \chi C_{15}^p \\ C_{15}^e - \chi C_{15}^p & C_{55}^e - \chi C_{55}^p \end{pmatrix} \begin{Bmatrix} d\bar{\varepsilon}_x^{(i)k} \\ d\bar{\varepsilon}_{zx}^{(i)k} \end{Bmatrix}. \tag{26}$$

Under hygrothermal conditions, the incremental elastoplastic stress-strain relations of the kth layer for the fiber-reinforced laminated beam are

$$\begin{Bmatrix} d\sigma_x^{(i)k} \\ d\tau_{zx}^{(i)k} \end{Bmatrix} = \begin{pmatrix} Q_{11}^k & Q_{15}^k \\ Q_{15}^k & Q_{55}^k \end{pmatrix} \begin{Bmatrix} d\bar{\varepsilon}_x^{(i)k} - \vartheta_x^k dT - \gamma_x^k dc \\ d\bar{\varepsilon}_{zx}^{(i)k} \end{Bmatrix}, \tag{27}$$

where $\vartheta_x^k = \vartheta_{11}\cos^2\theta_k + \vartheta_{22}\sin^2\theta_k$, and $\gamma_x^k = \gamma_{11}\cos^2\theta_k + \gamma_{22}\sin^2\theta_k$. $d\sigma_x^{(i)k}$, $d\tau_{zx}^{(i)k}$ denote the normal stress and shear stress increments of any points in the laminated beam, respectively, and Q_{ij}^k denotes the stiffness factor of the fiber-reinforced materials in the global coordinate. Denote θ_k as the playing angle of the kth layer, ϑ_{11}, ϑ_{22} as the thermal expansion coefficients in the longitudinal and lateral direction of the orthotropic material, and γ_{11}, γ_{22} as the humidity expansion coefficients. dT is the variation of the temperature and dc is the wet variation, which is defined as the ratio of the incremental mass dM after moisture absorption to the dry mass M.

According to the (25) and (27), the incremental membrane stress resultants $dN^{(i)L}$, the shear stress resultants $dQ^{(i)L}$ and stress couples $dM^{(i)L}$ of the fiber-reinforced laminated beam can be written as

$$\begin{bmatrix} dN^{(i)L} \\ dQ^{(i)L} \\ dM^{(i)L} \end{bmatrix} = \begin{pmatrix} A_1^{(i)L} & A_2^{(i)L} & B_1^{(i)L} \\ A_2^{(i)L} & A_3^{(i)L} & B_2^{(i)L} \\ B_1^{(i)L} & B_2^{(i)L} & D_1^{(i)L} \end{pmatrix} \begin{Bmatrix} d\varepsilon_x^{(i)} \\ d\varepsilon_{zx}^{(i)} \\ d\kappa_x^{(i)} \end{Bmatrix} - \begin{Bmatrix} dN_T^{(i)} \\ dQ_T^{(i)} \\ dM_T^{(i)} \end{Bmatrix}, \tag{28}$$

where

$$\begin{aligned} dN_T^{(i)} &= \int_{\Omega^{(i)e}} Q_{11}^k(\vartheta_x^k dT + \gamma_x^k dc)\,dz, & A_1^{(i)e} &= \int_{\Omega^{(i)e}} Q_{11}^k dz, & B_1^{(i)L} &= \int_{\Omega^{(i)e}} Q_{11}^k z\,dz, \\ dQ_T^{(i)} &= \int_{\Omega^{(i)e}} \eta Q_{15}^k(\vartheta_x^k dT + \gamma_x^k dc)\,dz, & A_2^{(i)L} &= \int_{\Omega^{(i)e}} Q_{15}^k dz, & B_2^{(i)L} &= \int_{\Omega^{(i)e}} Q_{15}^k z\,dz, \\ dM_T^{(i)} &= \int_{\Omega^{(i)e}} Q_{11}^k(\vartheta_x^k dT + \gamma_x^k dc)z\,dz, & A_3^{(i)L} &= \int_{\Omega^{(i)e}} \eta Q_{55}^k dz, & D_1^{(i)L} &= \int_{\Omega^{(i)e}} Q_{11}^k z^2 dz, \end{aligned}$$

where the last term of (28) is the stress resultants and couples resulting from the hygrothermal conditions. η denotes the shear stress modified coefficient, which is assumed as $\eta = 5/6$. As only cross-ply beams are considered in this paper, $Q_{15}^k = 0$ and $A_2^{(i)e} = B_2^{(i)e} = 0$.

The elastic constitutive relations of orthotropic piezoelectric layers can be described as

$$\begin{Bmatrix} \sigma_x^{(i)p} \\ \tau_{zx}^{(i)p} \end{Bmatrix} = \begin{pmatrix} Q_{11}^p & 0 \\ 0 & Q_{55}^p \end{pmatrix} \begin{Bmatrix} \bar{\varepsilon}_x^{(i)} \\ \bar{\varepsilon}_{xz}^{(i)} \end{Bmatrix} - \begin{pmatrix} 0 & e_{31} \\ 0 & 0 \end{pmatrix} \begin{Bmatrix} E_x^{(i)} \\ E_z^{(i)} \end{Bmatrix} - \begin{Bmatrix} \varsigma \\ 0 \end{Bmatrix} \Delta T, \tag{29}$$

$$\boldsymbol{D}^{(i)} = \begin{Bmatrix} D_x^{(i)} \\ D_z^{(i)} \end{Bmatrix} = \begin{pmatrix} 0 & 0 \\ e_{31} & 0 \end{pmatrix} \begin{Bmatrix} \bar{\varepsilon}_x^{(i)} \\ \bar{\varepsilon}_{xz}^{(i)} \end{Bmatrix} + \begin{pmatrix} t_{11} & 0 \\ 0 & t_{33} \end{pmatrix} \begin{Bmatrix} E_x^{(i)} \\ E_z^{(i)} \end{Bmatrix} = \boldsymbol{e} \cdot \begin{Bmatrix} \bar{\varepsilon}_x^{(i)} \\ \bar{\varepsilon}_{xz}^{(i)} \end{Bmatrix} + \boldsymbol{t} \cdot \boldsymbol{E}^{(i)}, \tag{30}$$

where $\sigma_x^{(i)p}$ and $\tau_{xz}^{(i)p}$ are the stress components of the piezoelectric layer, ς is the heat stress coefficient, $D_x^{(i)}$ and $D_z^{(i)}$ are the electric displacement components, $E_x^{(i)}$ and $E_z^{(i)}$ are the electric-field intensity components, Q_{ij}^p is the elastic constant, e_{ij} is the piezoelectric stress constant, and t_{ij} are dielectric constants.

It is assumed that only the electric field component $E_z^{(i)}$ throughout the thickness direction is applied on the piezoelectric layers. Denoting $V_T^{(i)}$, $V_B^{(i)}$ and $E_T^{(i)}$, $E_B^{(i)}$ as the electric voltages and the electric-field intensity on the upper and down surface, respectively, then the following relations are obtained

$$E_T^{(i)} = V_T^{(i)}/h^p, \quad E_B^{(i)} = V_B^{(i)}/h^p. \tag{31}$$

According to (29) and (23), the membrane stress resultants $N^{(i)p}$, shear stress resultants $Q^{(i)p}$ and stress couples $M^{(i)p}$ of the piezoelectric layers can be written as

$$\begin{bmatrix} N^{(i)p} \\ Q^{(i)p} \\ M^{(i)p} \end{bmatrix} = \begin{pmatrix} A_1^{(i)p} & A_2^{(i)p} & B_1^{(i)p} \\ A_2^{(i)p} & A_3^{(i)p} & B_2^{(i)p} \\ B_1^{(i)p} & B_2^{(i)p} & D_1^{(i)p} \end{pmatrix} \begin{Bmatrix} \varepsilon_x^{(i)} \\ \varepsilon_{zx}^{(i)} \\ \kappa_x^{(i)} \end{Bmatrix} - \begin{Bmatrix} N_a^{(i)p} \\ 0 \\ M_a^{(i)p} \end{Bmatrix} - \begin{Bmatrix} N_e^{(i)p} \\ 0 \\ M_e^{(i)p} \end{Bmatrix}, \tag{32}$$

where the last term is the change of stress resultants and stress couples after applying voltages on piezoelectric layer, and

$$\begin{aligned} N_a^{(i)p} &= \int_{\Omega^{(i)p}} \varsigma \Delta T \, dz, & A_1^{(i)p} &= \int_{\Omega^{(i)p}} Q_{11}^p dz, & B_1^{(i)p} &= \int_{\Omega^{(i)p}} Q_{11}^p z \, dz, \\ M_a^{(i)p} &= \int_{\Omega^{(i)p}} \varsigma \Delta T z \, dz, & A_2^{(i)p} &= 0, & B_2^{(i)p} &= 0, \\ N_e^{(i)p} &= \int_{\Omega^{(i)p}} \boldsymbol{e} \cdot \boldsymbol{E}^{(i)} dz, & A_3^{(i)p} &= \int_{\Omega^{(i)p}} Q_{55}^p dz, & D_1^{(i)p} &= \int_{\Omega^{(i)p}} z^2 Q_{11}^p dz, \\ M_e^{(i)p} &= \int_{\Omega^{(i)p}} \boldsymbol{e} \cdot \boldsymbol{E}^{(i)} z \, dz. \end{aligned} \tag{33}$$

From (27) and (32), the membrane stress resultants $N^{(i)}$, shear stress resultants $Q^{(i)}$ and stress couples $M^{(i)}$ of piezoelectric laminated beam can be written as

$$\begin{aligned} \begin{bmatrix} N^{(i)} \\ Q^{(i)} \\ M^{(i)} \end{bmatrix} &= \begin{bmatrix} N^{(i)e} \\ Q^{(i)e} \\ M^{(i)e} \end{bmatrix} + \begin{bmatrix} N^{(i)p} \\ Q^{(i)p} \\ M^{(i)p} \end{bmatrix} \\ &= \begin{pmatrix} A_1^{(i)} & A_2^{(i)} & B_1^{(i)} \\ A_2^{(i)} & A_3^{(i)} & B_2^{(i)} \\ B_1^{(i)} & B_2^{(i)} & D_1^{(i)} \end{pmatrix} \begin{Bmatrix} \varepsilon_x^{(i)} \\ \varepsilon_{zx}^{(i)} \\ \kappa_x^{(i)} \end{Bmatrix} - \begin{Bmatrix} N_b^{(i)} \\ Q_b^{(i)} \\ M_b^{(i)} \end{Bmatrix} \\ &= \begin{pmatrix} A_1^{(i)e} + A_1^{(i)p} & A_2^{(i)e} + A_2^{(i)p} & B_1^{(i)e} + B_1^{(i)p} \\ A_2^{(i)e} + A_2^{(i)p} & A_3^{(i)e} + A_3^{(i)p} & B_2^{(i)e} + B_2^{(i)p} \\ B_1^{(i)e} + B_1^{(i)p} & B_2^{(i)e} + B_2^{(i)p} & D_1^{(i)e} + D_1^{(i)p} \end{pmatrix} \begin{Bmatrix} \varepsilon_x^{(i)} \\ \varepsilon_{zx}^{(i)} \\ \kappa_x^{(i)} \end{Bmatrix} - \begin{Bmatrix} N_T^{(i)} + N_a^{(i)p} + N_e^{(i)p} \\ Q_T^{(i)} \\ M_T^{(i)} + M_a^{(i)p} + M_e^{(i)p} \end{Bmatrix}, \end{aligned} \tag{34}$$

where

$$N_b^{(i)} = N_T^{(i)} + N_a^{(i)p} + N_e^{(i)p}, \quad Q_b^{(i)} = Q_T^{(i)}, \quad M_b^{(i)} = M_T^{(i)} + M_a^{(i)p} + M_e^{(i)p}. \tag{35}$$

According to the classical nonlinear theory of laminated plates, and in view of the effect of the shear stress resultants on the membrane stress resultants, the nonlinear equilibrium equations of the laminated beams with initial deflection are acquired as

$$N^{(i)}_{,x} - (Q^{(i)}\phi^{(i)})_{,x} = 0, \quad Q^{(i)}_{,x} + [N^{(i)}(w^{(i)}_{,x} + \tilde{w}^{(i)}_{,x})]_{,x} = 0, \quad Q^{(i)} - M^{(i)}_{,x} = 0. \tag{36}$$

When the axial load acting on the piezoelectric laminated beam increases by a small quantity dP, the incremental nonlinear equilibrium equations can be obtained as

$$\begin{aligned}
&dN^{(i)}_{,x} - Q^{(i)}_{,x}d\phi^{(i)} - dQ^{(i)}_{,x}\phi^{(i)} - dQ^{(i)}_{,x}d\phi^{(i)} - Q^{(i)}d\phi^{(i)}_{,x} - dQ^{(i)}\phi^{(i)}_{,x} - dQ^{(i)}d\phi^{(i)}_{,x} = 0,\\
&dQ^{(i)}_{,x} + dN^{(i)}_{,x}(w^{(i)}_{,x} + \tilde{w}^{(i)}_{,x}) + N^{(i)}_{,x}dw^{(i)}_{,x} + dN^{(i)}_{,x}dw^{(i)}_{,x} + dN^{(i)}(w^{(i)}_{,xx} + \tilde{w}^{(i)}_{,xx}) + N^{(i)}dw^{(i)}_{,xx} + dN^{(i)}dw^{(i)}_{,xx} = 0,\\
&dQ^{(i)} - dM^{(i)}_{,x} = 0.
\end{aligned} \tag{37}$$

By introducing the dimensionless parameters

$$\begin{aligned}
&\xi^{(i)} = \frac{x^{(i)}}{L^{(i)}}, \quad W^{(i)} = \frac{w^{(i)}}{h}, \quad U^{(i)} = \frac{u^{(i)}}{L}, \quad \varphi = \phi,\\
&\alpha_i = \frac{h^{(i)}}{h}, \quad \beta_i = \frac{L^{(i)}}{L}, \quad \lambda_i = \frac{L^{(i)}}{h}, \quad H = \frac{L}{h},\\
&\bar{A}^{(i)}_1 = \frac{A^{(i)}_1}{Kh}, \quad \bar{A}^{(i)}_3 = \frac{A^{(i)}_3}{Kh}, \quad \bar{B}^{(i)}_1 = \frac{B^{(i)}_1}{Kh^2}, \quad \bar{D}^{(i)}_1 = \frac{D^{(i)}_1}{Kh^3},\\
&\bar{N}^{(i)}_b = \frac{N^{(i)}_b}{Kh}, \quad \bar{M}^{(i)}_b = \frac{M^{(i)}_b}{Kh^2}, \quad \bar{P} = \frac{P}{Kh}, \quad \tilde{W}^{(i)} = \frac{\tilde{w}^{(i)}}{h}
\end{aligned}$$

and substituting them, together with (27) and (34), into (37), we obtain the dimensionless nonlinear equilibrium equations of the delaminated piezoelectric laminated beam with initial deflection under the action of the axial load P. They read as follows, where $i = 1, 2, 3, 4$:

$$\begin{aligned}
&\bar{A}^{(i)}_1\left[\frac{1}{\beta_i}dU^{(i)}_{,\xi\xi} + \frac{1}{\lambda^2_i}(W^{(i)}_{,\xi} + \tilde{W}^{(i)}_{,\xi})\,dW^{(i)}_{,\xi\xi} + \frac{1}{\lambda^2_i}(W^{(i)}_{,\xi\xi} + \tilde{W}^{(i)}_{,\xi\xi})\,dW^{(i)}_{,\xi} + \frac{1}{\lambda^2_i}dW^{(i)}_{,\xi\xi}dW^{(i)}_{,\xi}\right]\\
&\quad + \frac{\bar{B}^{(i)}_1}{\lambda_i}d\varphi^{(i)}_{,\xi\xi} - \bar{A}^{(i)}_3\varphi^{(i)}_{,\xi}\left(\frac{1}{\lambda_i}dW^{(i)}_{,\xi} + d\varphi^{(i)}\right) - \bar{A}^{(i)}_3\varphi^{(i)}\left(\frac{1}{\lambda_i}dW^{(i)}_{,\xi\xi} + d\varphi^{(i)}_{,\xi}\right)\\
&\quad - \bar{A}^{(i)}_3 d\varphi^{(i)}_{,\xi}\left(\frac{1}{\lambda_i}dW^{(i)}_{,\xi} + d\varphi^{(i)}\right) - \bar{A}^{(i)}_3 d\varphi^{(i)}\left(\frac{1}{\lambda_i}dW^{(i)}_{,\xi\xi} + d\varphi^{(i)}_{,\xi}\right) - \bar{Q}^{(i)}d\varphi^{(i)}_{,\xi} - \bar{Q}^{(i)}_{,\xi}d\varphi^{(i)} = 0,
\end{aligned}$$

$$\begin{aligned}
&\bar{A}^{(i)}_3\left(\frac{1}{\lambda_i}dW^{(i)}_{,\xi} + d\varphi^{(i)}\right) - \left[\bar{B}^{(i)}_1\left[\frac{1}{\lambda_i\beta_i}dU^{(i)}_{,\xi\xi} + \frac{1}{\lambda^3_i}(W^{(i)}_{,\xi} + \tilde{W}^{(i)}_{,\xi})\,dW^{(i)}_{,\xi\xi}\right.\right.\\
&\qquad \left.\left. + \frac{1}{\lambda^3_i}(W^{(i)}_{,\xi\xi} + \tilde{W}^{(i)}_{,\xi\xi})dW^{(i)}_{,\xi} + \frac{1}{\lambda^3_i}dW^{(i)}_{,\xi\xi}dW^{(i)}_{,\xi}\right] + \frac{\bar{D}^{(i)}_1}{\lambda^2_i}d\varphi^{(i)}_{,\xi\xi}\right] = 0,
\end{aligned} \tag{38}$$

$$\bar{A}_3^{(i)}\left(\frac{1}{\lambda_i}dW_{,\xi\xi}^{(i)}+d\varphi_{,\xi}^{(i)}\right)+\frac{1}{\lambda_i}\bar{N}^{(i)}dW_{,\xi\xi}^{(i)}+\frac{1}{\lambda_i}\bar{N}_{,\xi}^{(i)}dW_{,\xi}^{(i)}$$
$$+\frac{1}{\lambda_i}\left(W_{,\xi\xi}^{(i)}+\tilde{W}_{,\xi\xi}^{(i)}+dW_{,\xi\xi}^{(i)}\right)\left\{\bar{A}_1^{(i)}\left[\frac{1}{\beta_i}dU_{,\xi}^{(i)}+\frac{1}{\lambda_i^2}(W_{,\xi}^{(i)}+\tilde{W}_{,\xi}^{(i)})\,dW_{,\xi}^{(i)}+\frac{1}{2\lambda_i^2}dW_{,\xi}^{(i)2}\right]+\frac{\bar{B}_1^{(i)}}{\lambda_i}d\varphi_{,\xi}^{(i)}\right\}$$
$$+\frac{1}{\lambda_i}\left(W_{,\xi}^{(i)}+\tilde{W}_{,\xi}^{(i)}+dW_{,\xi}^{(i)}\right)\left\{\bar{A}_1^{(i)}\left[\frac{1}{\beta_i}dU_{,\xi\xi}^{(i)}+\frac{1}{\lambda_i^2}(W_{,\xi}^{(i)}+\tilde{W}_{,\xi}^{(i)})\,dW_{,\xi\xi}^{(i)}\right.\right.$$
$$\left.\left.+\frac{1}{\lambda_i^2}(W_{,\xi\xi}^{(i)}+\tilde{W}_{,\xi\xi}^{(i)})\,dW_{,\xi}^{(i)}+\frac{1}{\lambda_i^2}dW_{,\xi\xi}^{(i)}dW_{,\xi}^{(i)}\right]+\frac{\bar{B}_1^{(i)}}{\lambda_i}d\varphi_{,\xi\xi}^{(i)}\right\}$$
$$=0. \quad (39)$$

Now we consider the dimensionless boundary conditions, continuity conditions of displacements and equilibrium conditions of moments and forces of delaminated piezoelectric laminated beams.

Assuming that the both ends of piezoelectric laminated beams are clamped with in-plane movable, the dimensionless boundary conditions are

$$\begin{aligned} &dW^{(1)}(0)=0, \quad d\bar{N}^{(1)}(0)=-d\bar{P}, \quad d\varphi^{(1)}(0)=0,\\ &dW^{(4)}(1)=0, \quad d\bar{N}^{(4)}(1)=-d\bar{P}, \quad d\varphi^{(4)}(1)=0. \end{aligned} \quad (40)$$

The dimensionless continuity conditions of displacements are

$$\begin{aligned} &dU^{(2)}(0)=dU^{(1)}(1)-\frac{1-\alpha_2}{2H}d\varphi^{(1)}(1), \quad dU^{(3)}(0)=dU^{(1)}(1)+\frac{1-\alpha_3}{2H}d\varphi^{(1)}(1),\\ &dW^{(1)}(1)=dW^{(2)}(0)=dW^{(3)}(0), \qquad d\varphi^{(1)}(1)=d\varphi^{(2)}(0)=d\varphi^{(3)}(0),\\ &dU^{(2)}(1)=dU^{(4)}(0)-\frac{1-\alpha_2}{2H}d\varphi^{(4)}(0), \quad dU^{(3)}(1)=dU^{(4)}(0)+\frac{1-\alpha_3}{2H}d\varphi^{(4)}(0),\\ &dW^{(4)}(0)=dW^{(2)}(1)=dW^{(3)}(1), \qquad d\varphi^{(4)}(0)=d\varphi^{(2)}(1)=d\varphi^{(3)}(1). \end{aligned} \quad (41)$$

The dimensionless equilibrium conditions of moments and forces are

$$\begin{aligned} &d\bar{N}^{(1)}(1)=d\bar{N}^{(2)}(0)+d\bar{N}^{(3)}(0), \quad d\bar{Q}^{(1)}(1)=d\bar{Q}^{(2)}(0)+d\bar{Q}^{(3)}(0),\\ &d\bar{M}^{(1)}(1)=d\bar{M}^{(2)}(0)+d\bar{M}^{(3)}(0)-\frac{1-\alpha_2}{2}d\bar{N}^{(2)}(0)+\frac{1-\alpha_3}{2}d\bar{N}^{(3)}(0),\\ &d\bar{N}_4(0)=d\bar{N}^{(2)}(1)+d\bar{N}^{(3)}(1), \qquad d\bar{Q}_4(0)=d\bar{Q}^{(2)}(1)+d\bar{Q}^{(3)}(1),\\ &d\bar{M}_4(0)=d\bar{M}^{(2)}(1)+d\bar{M}^{(3)}(1)-\frac{1-\alpha_2}{2}d\bar{N}^{(2)}(1)+\frac{1-\alpha_3}{2}d\bar{N}^{(3)}(1). \end{aligned} \quad (42)$$

4. Analysis of energy release rate along delamination front

In order to analyze the fatigue growth of the delamination, the stress field near the delamination front must be known. In fact, it is quite a tough task to analyze the stress of the delamination front due to its singularity. However, the energy release rate, which indicates intensity of stress fields near delamination

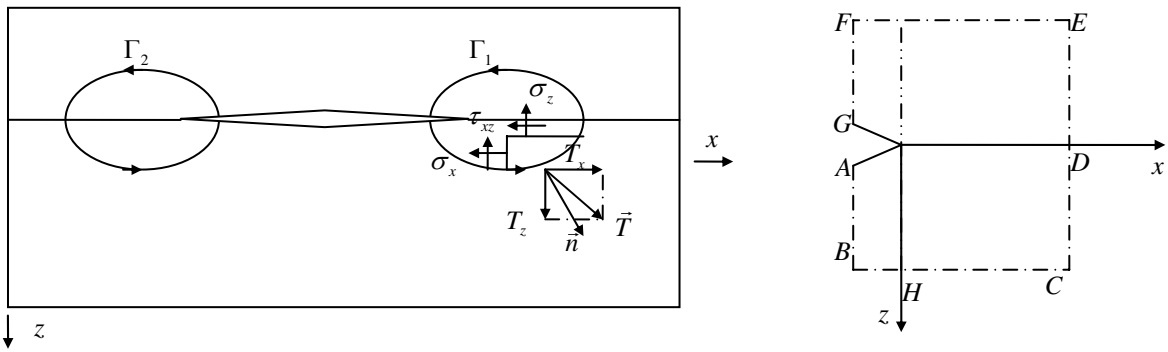

Figure 2. Left: the path of the J integral along the delamination front. Right: a rectangular path of the J integral along the delamination front.

front, can be determined. As a result, most researches of delamination growth were carried out by investigating the energy release rate. Rice [1968] proposed the J integral to describe the intensity of the stress and strain field in the vicinity of the crack tip for the elastoplastic structure. The J integral denotes the energy released when the crack tip propagates at a unit distance in the direction along the crack surface, that is, the energy release rate of an elastoplastic crack. In the case of linear elastic, the J integral is equal to the energy release rate G.

Rice [1968] defined the J integral of a two-dimensional crack as

$$J = \int_{\Gamma} \left(U dz - T_i \frac{\partial u_i}{\partial x} ds \right), \tag{43}$$

where $U = \int_0^{\varepsilon_{ij}} \sigma_{ij} d\varepsilon_{ij}$ is the strain energy density, $T_i = \sigma_{ij} n_j$ is the stress tensor along the length element ds, u_i is the displacement vector, $\vec{n}$ is the unit external normal vector, and Γ is an arbitrary contour surrounding the crack tip as shown in Figure 2, left. The counter-clockwise is supposed as the positive direction of the arc s.

Based on the law of conservation of energy, the generalized piezoelectric J integral was defined in [Pak and Herrmann 1986; Pak 1990; Zuo and Sih 2000], including piezoelectric effects and was proved to be independent of the choice of a contour:

$$J = \int_{\Gamma} (H n_k - T_i u_{i,k} + D_j n_j E_k) \, d\Gamma, \tag{44}$$

where $H = U - E_j D_j$.

Offsetting the global coordinate system oxz to the right end of the delamination and taking the integral path surrounding the right end of the delamination as a rectangle as shown in Figure 2, right, then yields (see [Li et al. 2011])

$$J_1 = J_{AB} + J_{BC} + J_{CD} + J_{DE} + J_{EF} + J_{FG}. \tag{45}$$

Noting that along the path AB, CE and FG, $dx = 0$ and for the path BC and EF, $dz = 0$.

5. Solution methodology

It is impossible to seek an analytic solution satisfying (38)–(39) and all the conditions (40)–(42). We therefore employ the finite difference method to discretize the coordinate variable. The considered domain of each region is $0 \le \xi_1, \xi_2, \xi_3, \xi_4 \le 1$ and each region is divided into M sections. All derivative terms relative to the space coordinate variable are replaced by difference scheme for the nonlinear equilibrium equations (38)–(39) and solution-determining conditions (40)–(42). The difference schemes of all derivative terms in these equations as $dU^{(i)}_{,\xi}$, $dU^{(i)}_{,\xi\xi}$, $dW^{(i)}_{,\xi}$, $dW^{(i)}_{,\xi\xi}$, $d\varphi^{(i)}_{,\xi}$, $d\varphi^{(i)}_{,\xi\xi}$ can be easily obtained. Given that C^p_{ij} in (26) relates to the current stresses and strains, the value of $A^{(i)}_1$, $A^{(i)}_3$, $B^{(i)}_1$, $D^{(i)}_1$ can not be obtained by direction integration along the thickness of the beam. Therefore, we discrete C^p_{ij} along the thickness of the beam, and divide the thickness into n uniform parts. Then by setting $z_k = -h/2 + kh/n$, the values of $A^{(i)}_1$, $A^{(i)}_3$, $B^{(i)}_1$, $D^{(i)}_1$ can be obtained by using the compound trapezoid formula. The compound trapezoid formula is also utilized to work out the J integral value, where the partial derivations of the displacements are approximated by difference schemes.

Then the nonlinear terms of governing equations and corresponding conditions are linearized and can be written as

$$(X \cdot Y)_j = (X)_j (Y)_{j_p}, \tag{46}$$

in which $(Y)_{J_p}$ is the value of the former iterative step. For the primary iteration, secondary extrapolation method is introduced to obtain the value of $(Y)_{J_p}$, that is

$$(Y)_{j_p} = A(Y)_{j-1} + B(Y)_{j-2} + C(Y)_{j-3}. \tag{47}$$

As for different iterations, the coefficients A, B and C are given by

$$\begin{aligned} &j=1: && A=1, && B=0, && C=0,\\ &j=2: && A=2, && B=-1, && C=0,\\ &j\ge 3: && A=3, && B=-3, && C=1. \end{aligned} \tag{48}$$

The cubic nonlinear terms are treated by the same method as the quadratic nonlinearity.

6. Numerical results and discussion

To ensure the accuracy and effectiveness of the present approaches, buckling of the isotropic elastic delaminated beams is analyzed. Neglecting the initial deflection, hygrothermal effects, piezoelectric effects and nonlinearity, (38)–(39) degenerates to

$$\begin{aligned} &\frac{\bar{A}^{(i)}_1}{\beta_i} dU^{(i)}_{,\xi\xi} + \frac{\bar{B}^{(i)}_1}{\lambda_i} d\varphi^{(i)}_{,\xi\xi} = 0,\\ &\frac{\bar{A}^{(i)}_3}{\lambda_i} dW^{(i)}_{,\xi\xi} + \bar{A}^{(i)}_3 d\varphi^{(i)}_{,\xi} - \frac{\alpha_i \bar{P}_{cr} \bar{A}^{(i)}_1}{\lambda_i} dW^{(i)}_{,\xi\xi} = 0,\\ &\frac{\bar{A}^{(i)}_3}{\lambda_i} dW^{(i)}_{,\xi} + \bar{A}^{(i)}_3 d\varphi^{(i)} - \frac{\bar{B}^{(i)}_1}{\beta_i \lambda_i} dU^{(i)}_{,\xi\xi} - \frac{\bar{D}^{(i)}_1}{\lambda_i^2} d\varphi^{(i)}_{,\xi\xi} = 0 \quad (i = 1, 2, 3, 4), \end{aligned} \tag{49}$$

	Geometric parameters				
	$\beta_2 = 0.2$	$\beta_2 = 0.3$	$\beta_2 = 0.5$	$\beta_2 = 0.6$	$\beta_2 = 0.8$
[Li and Zhou 2000]	0.63758	0.61012	0.43127	0.33275	0.12437
present	0.64312	0.62135	0.44805	0.34107	0.13841

Table 1. Values of $\bar{P}_{cr}$ for different delaminated lengths: current method compared with [Li and Zhou 2000].

where $\bar{P}_{cr}$ is the critical load of the isotropic delaminated beam. By (49), in conjunction with the conditions (40)–(42), the critical buckling load can be obtained.

Table 1 shows the critical loads of delaminated isotropic beams obtained with the present approach and compares them with those in [Li and Zhou 2000], the material parameters and geometric parameters being the same. The close agreement observed lends credibility to the present method.

The constant K in (1) can be determined by a simple tension test, and then $\Sigma_{11}(= K)$ can be determined. In the following numerical examples, set $\tilde{\sigma}(\bar{\varepsilon}^p) = \Sigma_{11} + \Sigma_{11}(\bar{\varepsilon}^p)^{0.51}$, $a = 0.6$ and $c = 2K/3$.

Let the dimensionless initial deflections be

$$\tilde{W}^{(i)} = \frac{\tilde{W}_0}{\beta_i} \sin \xi\pi, \tag{50}$$

where $\tilde{W}_0$ is the amplitude of the initial deflection of the beam without delamination.

If there is no specific explanation, in the following numerical examples we select PZT-5A as the piezoelectric layers and the corresponding material parameters are $E_L = E_T = 61\,\text{GPa}$, $G_{LT} = 22.6\,\text{GPa}$, $G_{LZ} = G_{TZ} = 21.1\,\text{GPa}$, $\upsilon_{LT} = 0.35$, $e_{31} = 7.209\,\text{C/m}^2$, $V_T = V_B$. The material parameters of the laminated beam are adopted as $E_L = 181.0\,\text{GPa}$, $E_T = 10.3\,\text{GPa}$, $G_{LT} = G_{LZ} = 7.17\,\text{GPa}$, $G_{TZ} = 3.87\,\text{GPa}$, $\upsilon_{LT} = 0.28$, $\Sigma_{11} = 500\,\text{MPa}$, $\Sigma_{55} = 200\,\text{MPa}$, $\vartheta_{11} = 6.1 \times 10^{-6}\,\text{K}^{-1}$, $\vartheta_{22} = 30.3 \times 10^{-6}\,\text{K}^{-1}$, $\gamma_{11} = 0$, $\gamma_{22} = 0.6 \times 10^{-6}$. For the sake of simplification, in present study, both ambient temperature and moisture are assumed to have a uniform distribution and leave out the hygrothermal effects of the piezoelectric layers. The material properties are assumed to be independent of temperature and moisture. The slenderness ratio of the beams is $H = 10$ and all layers have same thickness. The stacking sequences of the fiber-reinforced beam are $[0°/90°/0°]_{10}$. To simplify, only the postbuckling and delamination growth of piezoelectric elastoplastic laminated beams with symmetrical delamination are investigated in the numerical examples.

Analysis of postbuckling for delaminated piezoelectric elastoplastic laminated beams under hygrothermal conditions. In the calculation examples, the influences of the yield stress, delamination sizes and depths, hygrothermal conditions and piezoelectric effects on the postbuckling of delaminated piezoelectric elastoplastic laminated beams are discussed respectively. When analyze the postbuckling problem, we set $\tilde{W}_0 = 0.1$. In the following figures, $\bar{P}/\bar{P}^*_{cr}$ is the ratio of the dimensionless axial load to the dimensionless critical load of the beam without delamination, and $W_0^{(3)}$ is the maximum dimensionless deflection of region 3.

Figure 3, left, shows the comparison of postbuckling behavior between delaminated piezoelectric elastic and elastoplastic laminated beams, when $\alpha_2 = 0.4$, $\beta_2 = 0.5$ and $V = \Delta T = \Delta c = 0$. It can be

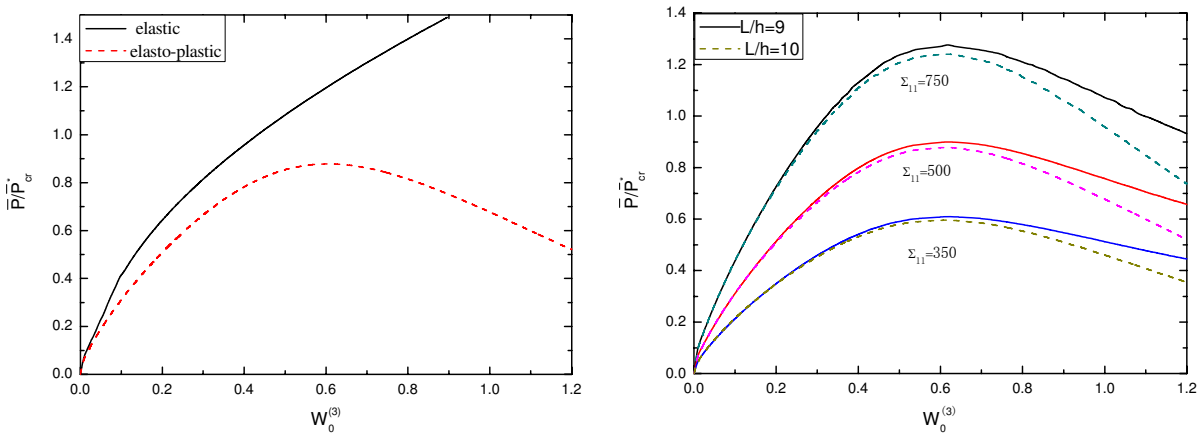

Figure 3. Left: comparison of postbuckling behavior between delaminated elastic and elastoplastic laminated beams. Right: Effect of yield stress on postbuckling behavior of delaminated piezoelectric elastoplastic laminated beams.

seen that the postbuckling curve of delaminated elastoplastic beams is quite different from the elastic beams. There exists a maximum in the elastoplastic postbuckling curve, which means that when the axial load surpasses the load carrying capacity, the deflection of the beams would increase rapidly.

For delaminated piezoelectric elastoplastic laminated beams with different slenderness ratio and yield stress, the variable curves of dimensionless load with the largest deflection of region 3 are presented in Figure 3, right, with $\alpha_2 = 0.4$, $\beta_2 = 0.5$ and $V = \Delta T = \Delta c = 0$. It is illustrated that the larger the slenderness ratio is, the more easily the delaminated piezoelectric elastoplastic laminated beams would yield, and the lower the load carrying capacity is. Note that when the yield stress of the fiber-reinforced material is less, the load carrying capacity of the delaminated piezoelectric elastoplastic beams is reduced.

Setting $\beta_2 = 0.5$ and $V = 0$, the effects of hygrothermal condition and delamination depths on the postbuckling curves of the delaminated piezoelectric elastoplastic laminated beams are depicted in Figure 4, left. As ΔT is much larger than Δc in practice, we take $\Delta T = 0 \sim 100^\circ$ C and $\Delta c = 0\% \sim 1\%$. Since magnitude of ϑ_x^k, γ_x^k are of the same order and the variation of humidity Δc is quite limited, so the humidity has little impact on the postbuckling curve and temperature is the main influencing factor. From the figure we can see that, with the same load, the increase of temperature decreases the load carrying capacity. That is because the increase of temperature is equivalent to an axial pressure, which reduces the stiffness of the beam. Under the same load, the beam with hygrothermal effects would yield a larger deflection than the beam in the thermostatic environments. In addition, the deeper the delamination is, the smaller the load carrying capacity is.

Under the action of the three types of electric load, the effects of delamination sizes on the postbuckling curves of the delaminated piezoelectric elastoplastic laminated beams with $\alpha_2 = 0.4$ are shown in Figure 4, right. The dimensionless control voltages are taken as $V = e_{31} V_T / Kh = 0.1$, 0 and -0.1, respectively, and the hygrothermal effects are not considered, namely, $\Delta T = \Delta c = 0$. It is indicated that, with the same geometric parameters and external load, acting a positive voltage on the beams is equivalent to an axial load, which leads to a larger deflection of the beams. It is just the opposite for the negative voltage. On the other hand, the larger the delamination size is, the lower the load carrying capacity is.

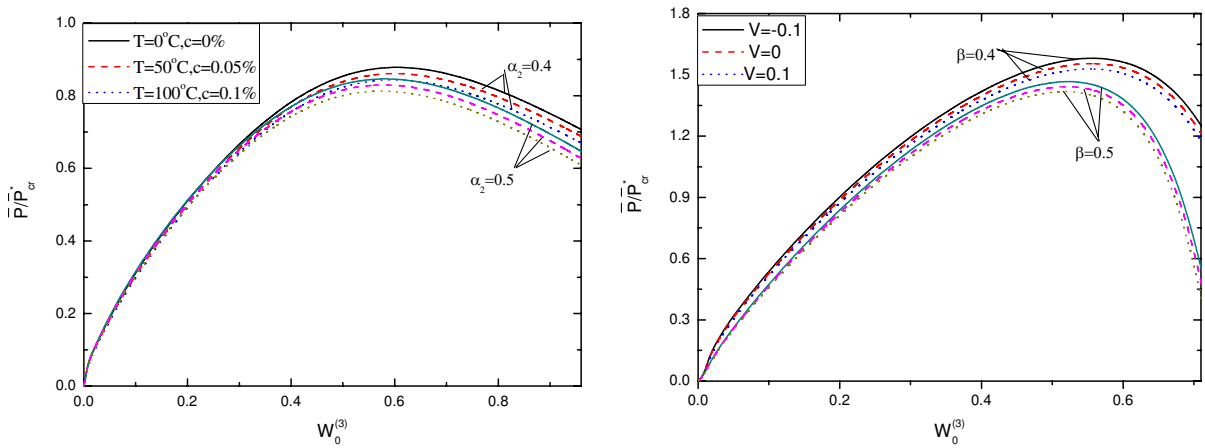

Figure 4. Left: effect of hygrothermal conditions on postbuckling behavior of delaminated piezoelectric elastoplastic laminated beams. Right: effect of control voltage on postbuckling behavior of delaminated piezoelectric elastoplastic laminated beams.

Analysis of delamination growth for delaminated piezoelectric elastoplastic laminated beams under hygrothermal conditions. In the following calculation examples, the influences of the yield stress, delamination sizes and depths, hygrothermal conditions and piezoelectric effects on the energy release rate of delaminated piezoelectric elastoplastic laminated beams without initial deflections are discussed respectively. In the following figures, $\bar{J}(= J_1/Kh)$ is the dimensionless value of J integral along the right delamination front.

Figure 5, left, presents the variation curves of energy release rate for delaminated piezoelectric elastoplastic laminated beams with different slenderness ratio and yield stress, when $\alpha_2 = 0.4$, $\beta_2 = 0.5$ and $V = \Delta T = \Delta c = 0$. It can be observed that the larger the slenderness ratio is, the larger the value of

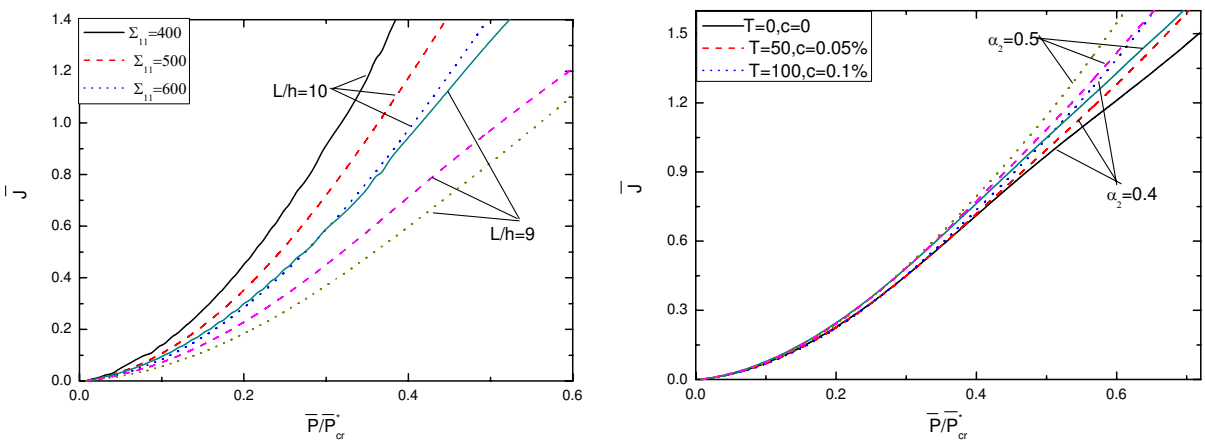

Figure 5. Left: effect of yield stress on energy release rate of delaminated piezoelectric elastoplastic laminated beams. Right: Effect of hygrothermal conditions on energy release rate of delaminated piezoelectric elastoplastic laminated beams.

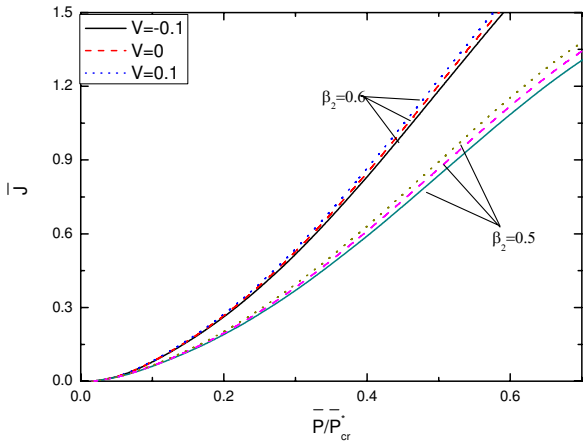

Figure 6. Effect of control voltage on energy release rate of delaminated piezoelectric elastoplastic laminated beams.

J integral, that is, the energy release rate, along the right delamination front is, which results in the delamination growth easier to occur. Moreover, when the yield stress of the fiber-reinforced material is larger, the J integral value along the right delamination front rises more quickly.

Setting $\beta_2 = 0.5$ and $V = 0$, the effects of hygrothermal condition and delamination depths on the energy release rate curves of the delaminated piezoelectric elastoplastic laminated beams are shown in Figure 5, right. It can be noticed that, with the same load, the increase of temperature make the energy release rate rise and the delamination propagate more easily. In addition, the deeper the delamination is, the larger the energy release rate is.

Subjected to three types of electric load, the effects of delamination sizes on the energy release rate of the delaminated piezoelectric elastoplastic laminated beams with $\alpha_2 = 0.4$ and $\Delta T = \Delta c = 0$ are presented in Figure 6. It is shown that, with the same geometric parameters and external load, applying a positive voltage leads to the energy release rate larger. However, the negative voltage is good for the stability of the delaminated beam. On the other hand, the larger the delamination size is, the larger the energy release is and the delamination growth is easier to occur.

7. Conclusions

The postbuckling and delamination growth for delaminated piezoelectric elastoplastic laminated beams under hygrothermal conditions are investigated in this paper. The numerical solutions are presented by using the finite difference method and the iteration method. The main conclusions can be drawn as follows. Under the same axial load, the postbuckling behavior of a delaminated elastic-plastic laminated beam is quite different with that of the delaminated elastic laminated beam and there is a load carrying capacity for the delaminated elastic-plastic laminated beam. With smaller yield stress, larger slenderness ratio, deeper and larger delamination, the load carrying capacity of the delaminated piezoelectric elastoplastic beam is lower. The effects of temperature increasing and positive voltage are equivalent to the axial pressures, which lead to the larger deformation of the beam and have a detrimental effect on the stability of the delaminated beams. The larger yield stress of the fiber-reinforce material makes

the energy release rate rise more quickly. When the slenderness ratio of the delaminated piezoelectric elastoplastic laminated beam, the external axial load, the increase of the temperature and the positive voltage are larger, and the delamination is deeper or larger, the energy release rates are larger and the delamination growth is easier to occur.

Acknowledgements

This project is supported by the National Natural Science Foundation of China (No. 11072076).

References

[Davidson et al. 2000] B. D. Davidson, S. J. Gharibian, and L. J. Yu, "Evaluation of energy release rate-based approaches for predicting delamination growth in laminated composites", *Int. J. Fract.* **105**:4 (2000), 343–365.

[Li and Zhou 2000] D. Li and J. Zhou, "Buckling analysis of delaminated beam for the higher-order shear deformation theory", *Acta Mech. Solida Sin.* **2000**:3 (2000), 225–233.

[Li et al. 2011] Y. L. Li, Y. M. Fu, and Y. Q. Mao, "Analysis of delamination fatigue growth for delaminated piezoelectric elasto-plastic laminated beams under hygrothermal conditions", *Compos. Struct.* **93**:2 (2011), 889–901.

[Münch and Ousset 2002] A. Münch and Y. Ousset, "Numerical simulation of delamination growth in curved interfaces", *Comput. Methods Appl. Mech. Eng.* **191**:19-20 (2002), 2073–2095.

[Nilsson et al. 2001] K.-F. Nilsson, L. E. Asp, J. E. Alpman, and L. Nystedt, "Delamination buckling and growth for delaminations at different depths in a slender composite panel", *Int. J. Solids Struct.* **38**:17 (2001), 3039–3071.

[Pak 1990] Y. E. Pak, "Crack extension force in a piezoelectric material", *J. Appl. Mech.* (*ASME*) **57**:3 (1990), 647–653.

[Pak and Herrmann 1986] Y. E. Pak and G. Herrmann, "Conservation laws and the material momentum tensor for the elastic dielectric", *Int. J. Eng. Sci.* **24**:8 (1986), 1365–1374.

[Park and Sankar 2002] O. Park and B. V. Sankar, "Crack-tip force method for computing energy release rate in delaminated plates", *Compos. Struct.* **55**:4 (2002), 429–434.

[Pi and Bradford 2003] Y.-L. Pi and M. A. Bradford, "Elasto-plastic buckling and postbuckling of arches subjected to a central load", *Comput. Struct.* **81**:18–19 (2003), 1811–1825.

[Rice 1968] J. R. Rice, "A path independent integral and the approximate analysis of concentration by notches and cracks", *J. Appl. Mech.* (*ASME*) **35**:2 (1968), 397–386.

[Shen 2001] H.-S. Shen, "Postbuckling of shear deformable laminated plates with piezoelectric actuators under complex loading conditions", *Int. J. Solids Struct.* **38**:44–45 (2001), 7703–7721.

[Shen 2002] H.-S. Shen, "Hygrothermal effects on the postbuckling of axially loaded shear deformable laminated cylindrical panels", *Compos. Struct.* **56**:1 (2002), 73–85.

[Simha et al. 2008] N. K. Simha, F. D. Fischer, G. X. Shan, C. R. Chen, and O. Kolednik, "J-integral and crack driving force in elastic-plastic materials", *J. Mech. Phys. Solids* **56**:9 (2008), 2876–2895.

[Tafreshi 2006] A. Tafreshi, "Delamination buckling and postbuckling in composite cylindrical shells under combined axial compression and external pressure", *Compos. Struct.* **72**:4 (2006), 401–418.

[Tian et al. 2009] Y. P. Tian, Y. M. Fu, and Y. Wang, "Nonlinear dynamic response of piezoelectric elasto-plastic laminated plates with damage", *Compos. Struct.* **88**:2 (2009), 169–178.

[Wang and Qiao 2004] J. Wang and P. Qiao, "On the energy release rate and mode mix of delaminated shear deformable composite plates", *Int. J. Solids Struct.* **41**:9–10 (2004), 2757–2779.

[Yang et al. 2002] W. Yang, S. Zhang, and Y. Ma, "Theoretical research of crack tip J-integral for orthotropic composite plate", *J. Taiyuan Heavy Mach. Inst.* **2002**:3 (2002), 226–232.

[Yuan and Zheng 1990] Z.-P. Yuan and Y. Zheng, "A study on yield and flow of orthotropic materials", *Appl. Math. Mech.* **11**:3 (1990), 247–253.

[Zuo and Sih 2000] J. Z. Zuo and G. C. Sih, "Energy density theory formulation and interpretation of cracking behavior for piezoelectric ceramics", *Theor. Appl. Fract. Mech.* **34**:1 (2000), 17–33.

Received 24 Dec 2010. Revised 10 Apr 2011. Accepted 11 Apr 2011.

YING-LI LI: liyingli298@yahoo.com
State Key Lab of Advanced Design and Manufacturing for Vehicle Body, College of Mechanical and Vehicle Engineering, Hunan University, Changsha, 410082, China

YI-MING FU: fym_2581@hnu.cn
College of Mechanical and Vehicle Engineering, Hunan University, Changsha, 410082, China

HONG-LIANG DAI: hldai520@sina.com
College of Mechanical and Vehicle Engineering, Hunan University, Changsha, 410082, China

JOURNAL OF MECHANICS OF MATERIALS AND STRUCTURES

jomms.net

Founded by Charles R. Steele and Marie-Louise Steele

See http://jomms.net for submission guidelines.

JoMMS (ISSN 1559-3959) is published in 10 issues a year. The subscription price for 2012 is US $555/year for the electronic version, and $735/year (+$60 shipping outside the US) for print and electronic. Subscriptions, requests for back issues, and changes of address should be sent to Mathematical Sciences Publishers, Department of Mathematics, University of California, Berkeley, CA 94720–3840.

JoMMS peer-review and production is managed by EditFLOW® from Mathematical Sciences Publishers.

PUBLISHED BY

mathematical sciences publishers

http://msp.org/

A NON-PROFIT CORPORATION

Typeset in LaTeX

Journal of Mechanics of Materials and Structures

Volume 7, No. 1 January 2012